Food and Chemical Toxicology 130 (2019) 242–252

Contents lists available at ScienceDirect

Food and Chemical Toxicology

journal homepage: www.elsevier.com/locate/foodchemtox

Long-term iron exposure causes widespread molecular alterations associated with memory impairment in mice

Xian Wang[a,b], Jiafei Zhang[a,b], Li Zhou[b], Benhong Xu[b], Xiaohu Ren[b], Kaiwu He[b], Lulin Nie[b], Xiao Li[b], Jianjun Liu[b,***], Xifei Yang[b,**], Jing Yuan[a,*]

[a] Department of Occupational and Environmental Health and Key Laboratory of Environment and Health, Ministry of Education & Ministry of Environmental Protection, and State Key Laboratory of Environmental Health (Incubating), School of Public Health, Tongji Medical College, Huazhong University of Science and Technology, Hangkong Road 13, Wuhan, 430030, Hubei, PR China

[b] Key Laboratory of Modern Toxicology of Shenzhen, Shenzhen Center for Disease Control and Prevention, Shenzhen, 518055, Guangdong, PR China

ARTICLE INFO

Keywords:
Iron
Neurotoxicity
Proteomics
Memory

ABSTRACT

Limited literature available indicates the neurotoxic effects of excessive iron, however, a deep understanding of iron neurotoxicity needs to be developed. In this study, we evaluated the toxic effects of excessive iron on learning and cognitive function in long-term iron exposure (oral, 10 mg/L, 6 months) of mice by behavioral tests including novel object recognition test, step-down passive avoidance test and Morris water maze test, and further analyzed differential expression of hippocampal proteins. The behavioral tests consistently showed that iron treatment caused cognitive defects of the mice. Proteomic analysis revealed 66 differentially expressed hippocampal proteins (30 increased and 36 decreased) in iron-treated mice as compared with the control ones. Bioinformatics analysis showed that the dysregulated proteins mainly included: synapse-associated proteins (i.e. synaptosomal-associated protein 25 (SNAP25), complexin-1 (CPLX1), vesicle-associated membrane protein 2 (VAMP2), neurochondrin (NCDN)); mitochondria-related proteins (i.e. ADP/ATP translocase 1 (SLC25A4), 14-3-3 protein zeta/delta (YWHAZ)); cytoskeleton proteins (i.e. neurofilament light polypeptide (NEFL), tubulin beta-2B chain (TUBB2B), tubulin alpha-4A chain (TUBA4A)). The findings suggest that the dysregulations of synaptic, mitochondrial, and cytoskeletal proteins may be involved in iron-triggered memory impairment. This study provides new insights into the molecular mechanisms of iron neurotoxicity.

1. Introduction

Iron is a necessary microelement in human body. It plays important roles in many biological processes of the brain tissue, including DNA synthesis, myelination as well as neurotransmitter synthesis and metabolism (Schroder et al., 2013; Ward et al., 2014). Previous studies reported that human exposed to iron through iron in tap water, iron intake from food and use of iron pot (Andrade et al., 2017; Peto, 2010). A recent review outlines on the neurotoxic effects of excessive iron on cognition and neurodegeneration in animal models and humans (Agrawal et al., 2017).

It is well known that both transferrin (Tf) and transferrin receptor (TfR) play vital roles in iron homeostasis. The iron in bloodstream can be captured by Tf and transported to peripheral tissues, and then transported across blood brain barrier through brain microvascular endothelial cells (BMEC) via Tf-TfR and iron transport proteins divalent metal transporter-1 (DMT1) and ferroportin. The circulating iron-Tf complex can be captured by TfR on the membrane of BMEC, internalized via endocytosis, released to the cytoplasm of BMEC via DMT1 and exported into brain interstitial fluid via ferroportin. The iron bound to Tf can be taken up by other cells including astrocytes and neurons (Gao and Chang, 2014; Jiang et al., 2017; Ward et al., 2014). Several factors may lead to brain iron accumulation in addition to body iron stores which tend to increase with aging-related changes in the body, including inflammation, increased blood-brain barrier permeability, brain iron redistribution and abnormal iron homoeostasis (Conde and Streit, 2006; Farrall and Wardlaw, 2009). Besides, accumulating evidence indicates the correlation between iron deposition in specific brain regions and neurodegenerative diseases, such as Alzheimer's disease (AD), Parkinson's disease, and multiple sclerosis. The results

* Corresponding author.
** Corresponding author.
*** Corresponding author.
E-mail addresses: junii8@126.com (J. Liu), xifeiyang@gmail.com (X. Yang), jyuan@tjh.tjmu.edu.cn (J. Yuan).

https://doi.org/10.1016/j.fct.2019.05.038
Received 26 March 2019; Received in revised form 9 May 2019; Accepted 24 May 2019
Available online 25 May 2019

Abbreviations

ACAA2	3-ketoacyl-CoA thiolase, mitochondrial
ACADM	medium-chain specific acyl-CoA dehydrogenase
AD	Alzheimer's disease
ADCY9	adenylate cyclase type 9
APP	amyloid precursor protein
BP	biological process
CC	cellular component
CLDN11	claudin-11
CPLX1	complexin-1
Cplxs	complexins
FA	formic acid
GNG7	guanine nucleotide-binding protein G(I)/G(S)/G(O) subunit gamma-7
HPRT1	hypoxanthine-guanine phosphoribosyltransferase
KEGG	Kyoto Encyclopedia of Genes and Genomes
MF	molecular function
MT2	metallothionein-2
NCDN	neurochondrin
NEFL	neurofilament light polypeptide
NME2	nucleoside diphosphate kinase B
PLP1	myelin proteolipid protein
PRKCE	protein kinase C epsilon type
PS1	presenilin 1
RAB5A	Ras-related protein Rab-5A
RAB11A	Ras-related protein Rab-11A
RAN	GTP-binding nuclear protein Ran
RPLP2	60S acidic ribosomal protein P2
RPS24	40S ribosomal protein S24
SLC1A3	excitatory amino acid transporter 1
SLC1A6	excitatory amino acid transporter 4
SLC25A4	ADP/ATP translocase 1
SNAP25	synaptosomal-associated protein 25
SNARE	soluble N-ethylmaleimide-sensitive factor attachment protein receptors
SV	synaptic vesicle
TBST	Tris-buffered saline/0.1% Tween
TMT	Tandem Mass Tag
TUBA4A	tubulin alpha-4A chain
TUBB2B	tubulin beta-2B chain
VAMP2	vesicle-associated membrane protein 2
VARS	valine-tRNA ligase
YWHAZ	14-3-3 protein zeta/delta

from the Australian Imaging, Biomarkers and Lifestyle study found that the brain iron could combine with amyloid-β to accelerate AD progression (Ayton et al., 2017). A study from the German Center for Neurodegenerative Diseases examined the whole-brain iron levels in 25 idiopathic Parkinson's disease patients and 50 matched controls, and found an apparent increase of iron deposition in the dorsal substantia nigra (Acosta-Cabronero et al., 2017). Another prospective study reported that independent of tissue atrophy, iron alteration in the deep gray matter was related to the evolution of multiple sclerosis (Zivadinov et al., 2018). In addition, increased iron levels, especially in hippocampus, cortical areas, and basal ganglia were found to be linked to the cognitive dysfunction (Schroder et al., 2013).

Earlier animal studies showed that iron supplementation (orally or intraperitoneal injection) at different growth phases of rodents could induce memory deficits evaluated by various behavioral tests. For example, a study of male NMRI mice showed that comparing with the controls, mice treated orally with Fe^{2+} (37 mg/kg) on the postnatal days 10–12 displayed the impairments in radial arm maze learning when they were 3 months old (Fredriksson et al., 1999). Another study showed that adult male rats with iron treatment ($FeSO_4$, 3 mg/kg, intraperitoneal injection, for 5 consecutive days) exhibited significant learning impairments in a Morris water maze task (Maaroufi et al., 2009).

Although the evidence from *in-vitro* studies indicated that iron exposure could alter mitochondrial function of neurons, the mechanisms underlying iron-induced neurotoxicity remain unknown. A study on primary cultures of rat brain cortical neurons showed that after 24-h treatment with ferric ammonium citrate, 58 mitochondrial proteins were significantly altered when comparing with the control by using an unlabeled quantitative proteomics approach (Huang et al., 2018). Moreover, ferric ammonium citrate was found to induce mitochondrial fragmentation in HT-22 hippocampal neuron cells of mice, which was related to Ca^{2+}-mediated calcineurin signals or dephosphorylation of dynamin related protein 1 (Ser637) (Lee et al., 2016; Park et al., 2015). Besides, the regulation of brain iron homeostasis is a complex network, specially involving several important proteins (such as Tf, ferritin and ferroportin) which can affect the import, storage and export of iron (Chen et al., 2019). Iron dysregulation is any kind of deviation from homeostatic iron metabolism (Pretorius et al., 2018). Intracellular iron homeostasis within the brain is maintained by a balance of both iron uptake and release, which is precisely regulated. Iron homeostasis at the cellular level is mainly regulated by iron transporters TfR, DMT1, and ferroportin. The uneven distribution of TfR in cerebral endothelia is found to be responsible for the differences of iron concentrations in different brain regions (Gao and Chang, 2014). However, iron dysregulation does occasionally occur. It is known that the control of cellular iron homeostasis is a post-transcriptional regulatory action regarding iron-regulatory proteins (IRP) 1 and 2. IRPs as cytosolic RNA-binding proteins can bind to iron-responsive elements (IREs) that encode the proteins to regulate the translation or stability of these mRNAs. Iron deficiency can promote IRPs to bind to IREs and then facilitate the regulations of ferritin, ferroportin, TfR1 and DMT1, leading to increase in iron uptake and inhibition in iron storage and export. On the contrary, excessive iron can make the IRPs inactive, which induces the translations of ferritin and ferroportin but destroys the stabilities of TfR1 and DMT1 (Weinreb et al., 2013). In addition, excessive iron could induce oxidative stress via free radical production through Fenton reaction, damage the neuronal mitochondria, affect its energy production and even lead to impaired synaptic function (Schroder et al., 2013).

In the current study, mice exposure to iron underwent a series of behavioral tests to evaluate the cognitive function, and a Tandem Mass Tag (TMT) proteomic approach was used to identify the differences in the alterations of hippocampal proteins. Our findings may shed new light on the molecular mechanisms of iron neurotoxicity.

2. Materials and methods

2.1. Reagents

Iron (III) chloride hexahydrate, dithiothreitol, iodoacetamide, hydroxylamine were purchased from Sigma-Aldrich Corporation (St. Louis, MO, USA). Urea was purchased from GE Healthcare Life Sciences (Uppsala, Sweden). Halt™ Protease Inhibitor Cocktail (100X), formic acid (FA), triethylammonium bicarbonate, TMT sixplex™ Label Reagent Set, Pierce™ BCA protein assay kit, Electro-Chemi-Luminescence kit were purchased from Thermo Fisher Scientific (Rockford, IL, USA). Sequencing Grade Modified Trypsin was obtained from Promega Corporation (Madison, WI, USA). Radio Immunoprecipitation Assay lysis buffer was purchased from Beyotime Biotechnology (Beijing, China). Anti-β-actin (sc-47778) and anti-SNAP25 (ab41455) were purchased from Santa Cruz Biotechnology (Dallas, TX, USA) and Abcam (Cambridge, UK), respectively.

2.2. Animals and treatments

Male mice (strain: C57/BL6) were originally obtained from the Guangdong Medical Laboratory Animal Center (Guangdong, China). They were housed with a 12-h light-dark cycle and given *ad libitum* access to water and food. All experimental procedures were performed following the National Institutes of Health guide for the care and use of Laboratory animals (NIH Publications No. 8023, revised 1978) and were approved by the Ethics Committee of the Shenzhen Center for Disease Control and Prevention.

Mice aged 3 months were randomly assigned to control or iron-treated groups (15 mice in each group). The control mice were given a standard diet and drinking water. The iron-treated mice were fed a standard diet and drinking water containing 10 mg/L of iron for 6 consecutive months. The oral dosage of iron was selected based on a previous report (Railey et al., 2011). Subsequently, mice aged 9 months were subjected to a series of behavioral tests to assess their cognitive functions. The mice were continuously treated with iron when the behavioral tests were performed. After the completion of behavioral tests, brain tissues were dissected out and appropriately treated for further analysis.

2.3. Behavioral tests

Considering the counterbalances in the series of behavioral tests (including the novel object recognition test, step-down passive avoidance test and Morris water maze test), we took the certain measures. For instance, the series of behavioral tests in the mice were performed in turn. There was an interval of 2 days between each two tests of the designed behavioral tests. The behavioral tests in mice were conducted in a quiet testing room between 9:00 a.m. and 5:00 p.m. Moreover, experimenters were blind to the groups, and mice in iron-treated and control groups were randomly tested.

2.3.1. Novel object recognition test

To evaluate recognition memory, we carried out the novel object recognition test according to the method as described by Faraco et al. (2018). Briefly, on the first day of this test, mice (n = 15 per group) were allowed to move freely in an empty plastic box (length × width × height: 47.5 × 35 × 20 cm^3) for 5 min to adapt to the environment. Twenty-four hours after habituation, mice were allowed free exploration for 5 min in the same box with two identical objects. One hour later, one of the two objects was replaced by a novel object with similar size but different shape, and then the mice were allowed to stay in the same box for additional 5 min. Exploration time for each object was recorded and expressed as a percentage of total exploration time.

2.3.2. Step-down passive avoidance test

To evaluate aversive learning and memory in mice model, we performed step-down passive avoidance test as described previously (Zhou et al., 2019). The apparatus consisted of 5 rectangular plexiglass chambers (length × width × height: 15 × 15 × 46 cm^3) with a floor of steel rods spaced 0.8 cm apart, and then a wooden platform (4.5 cm in diameter) was positioned in the middle of the floor. Mice (n = 13 per group) underwent 2 trials in turn: a training trial and a test trial 24 h later. During the training session, mice were firstly placed on the floor made of steel rods to conduct the electrical shock (36 V, AC) for 5 min. During the test session, mice were placed on the platform with energized steel rods. The latency of step-down and number of errors within 5 min were recorded.

2.3.3. Morris water maze test

To evaluate spatial learning and memory of mice, we conducted Morris water maze test according to the previous method (Vorhees and Williams, 2006). The apparatus was composed of a circular pool (170 cm in diameter) filled with opaque water (made white with milk power, 30 cm in depth, 22 °C), and a white escape platform (10 cm in diameter) was placed 2 cm underwater. Mice (n = 13 per group) went through the navigation trial and the probe trial. During the navigation test, mice were trained to find the hidden platform 4 trials (1 min for each mouse to explore the platform/each trial) each day for 5 consecutive days. The mouse was taken to the platform and stayed there for 15 s, if it failed to find the platform within 1 min. Six days after the completion of training, the probe test was performed, i.e., mice were allowed to swim in the pool without the platform for 2 min. Various parameters were recorded, including probe time, the number of crossing movements, time spent in target quadrant, distance travelled in target quadrant, and swimming paths.

2.4. Proteomic analysis

2.4.1. Preparation of protein samples

Protein samples from the hippocampi of mice were prepared based on the previous method (Xu et al., 2018). Briefly, after intraperitoneally injected with 1% pentobarbital sodium (60 mg/kg), mice were sacrificed and then the hippocampus tissues were dissected and stored at −80 °C until use. Hippocampus tissues (4 mice each group) in 8 M urea in phosphate buffered saline buffer were lysed with ultrasonic homogenizer (SONICS & MATERIALS INC., NEWTOWN, CT, USA). The lysates were centrifuged, and protein concentration was determined with NanoDrop 2000/2000c spectrophotometers (Thermo Fisher Scientific, Waltham, MA, USA).

2.4.2. TMT labeling

The sample with 100 μg protein was treated with dithiothreitol, and then incubated with iodoacetamide. Samples were diluted with phosphate buffered saline (pH 8.0) (final concentration: 1 M urea), digested with 1:25 w/w trypsin/Lys-C at 37 °C overnight and acidified with 1% FA. After centrifugation, the supernatants were desalted with reversed-phase column (Oasis HLB; Waters, Milford, MA, USA), dried with vacuum concentrator, and then dissolved in triethylammonium bicarbonate. Peptides were labeled with the TMT reagents at room temperature for 1 h: TMT-126 for hippocampi of the control mice; TMT-131 for hippocampi of the iron-treated mice (n = 4 per group). Hydroxylamine was used to terminate the reactions. The labeled peptides from the control and iron-treated groups were mixed (n = 4), desalted, dried, and dissolved in 100 μL 0.1% FA.

2.4.3. High performance liquid chromatography (HPLC) separation

The labeled peptides were fractionated using a previously described procedure (Gokce et al., 2011). Briefly, peptides were loaded onto the Xbridge BEH300 C_{18} column (Waters, Milford, MA, USA) for HPLC (UltiMate 3000 UHPLC; Thermo Fisher Scientific, Waltham, MA, USA) separation. Fractions were collected, dried, dissolved in 20 μL 0.1% FA for further liquid chromatography (LC)-mass spectrometry (MS)/MS analysis.

2.4.4. LC-MS/MS analysis and database searching

Peptide analysis was conducted by LC-MS/MS according to a previous method (Xu et al., 2018). Briefly, UltiMate 3000 RSLCnano System (Thermo Fisher Scientific, Waltham, MA, USA) was directly interfaced with Thermo Q Exactive Benchtop mass spectrometer (Thermo Fisher Scientific, Waltham, MA, USA). Peptides were separated by an analytical capillary column (Upchurch, Oak Harbor, WA, USA) packed with C_{18} silica resin (Varian, Lexington, MA, USA).

The raw mass spectra were searched with the Uniprot-*Mus musculus* database (released in October 2018) using Proteome Discoverer 2.1 software (Thermo Fisher Scientific, Waltham, MA, USA). The search criteria were set based on a previous study (Xu et al., 2018).

2.4.5. Bioinformatics analysis

We used *t*-tests in the Perseus computational platform to compare log2-transformed scaled abundances of proteins between the control and iron-treated groups (Bereczki et al., 2018; Tyanova et al., 2016). *P* value was adjusted by false discovery rate controlling approach to reduce the number of false positives for multiple comparisons (Pike, 2011). Differentially expressed proteins were determined (requirements: adjusted $P < 0.05$ and fold change < 0.9 or > 1.1). GraphPad Prism 7.00 was used to make heat map and volcano plot. The identified proteins involved in molecular function (MF), cellular component (CC), biological process (BP), and Kyoto Encyclopedia of Genes and Genomes (KEGG) pathway were analyzed by DAVID Bioinformatics Resources 6.8 (https://david.ncifcrf.gov/). STRING database was used to analyze the protein-protein interaction, and the interaction network was visualized in Cytoscape version 3.7.0.

2.5. Western blot

Hippocampal proteins were prepared by Radio Immunoprecipitation Assay lysis buffer and then quantified with Pierce™ BCA protein assay kit. Afterwards, proteins samples were separated on 12% sodium dodecyl sulfate polyacrylamide gel electropheresis and transferred to polyvinylidene fluoride membranes. Membranes were blocked with 5% skim milk in Tris-buffered saline/0.1% Tween (TBST) buffer for 1 h at room temperature, and then incubated with anti-β-actin (1:3000) and anti-SNAP25 (1:3000) in TBST buffer overnight at 4 °C. The membrane was washed in TBST, incubated with anti-mouse or anti-rabbit IgG HRPs (1:3000) in TBST buffer for 1 h, washed again in TBST, and exposed with chemiluminescence reagents from an Electro-Chemi-Luminescence kit. Densitometry analysis of the Western blot protein was performed by using Image Processing and Analysis in Java (ImageJ) software (National Institutes of Health, Bethesda, Maryland, USA).

2.6. Statistical analysis

Data were expressed as mean ± SEM. Intergroup differences were evaluated by unpaired Student's *t* tests. Statistic analysis was performed by SPSS 12.0 software (Statistical Program for Social Sciences Inc., Chicago, IL, USA). Two-sided *P* values < 0.05 were considered statistically significant.

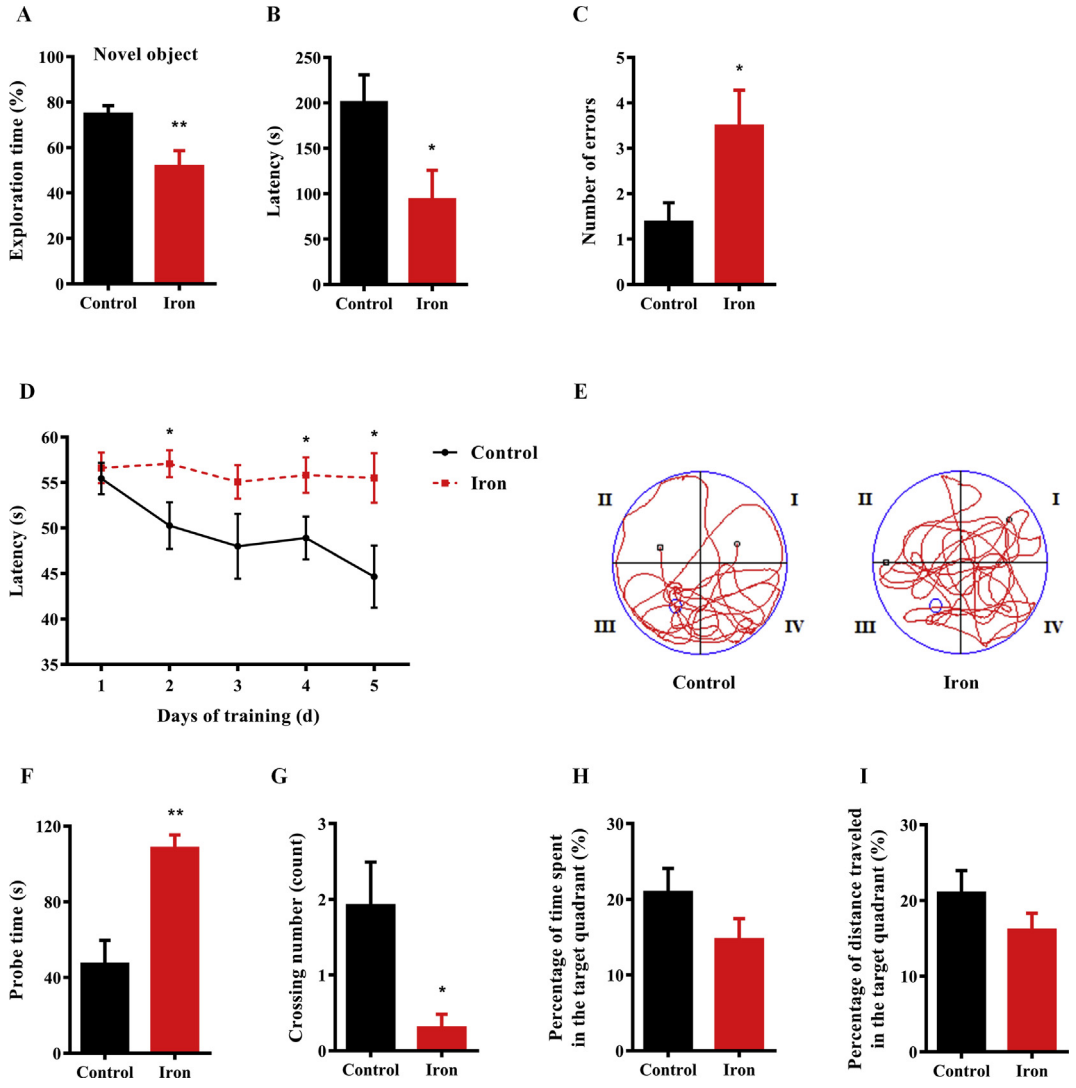

Fig. 1. Iron induced cognitive dysfunction in mice. A) Differences in the exploration time of novel object in novel object recognition test (n = 15 per group). B–C) The latency and number of errors in the step-down passive avoidance test (n = 13 per group). D) Escape latency in the Morris water maze training trials. E-I) Differences in representative tracks of movement patterns, probe time, the number of crossing movements, percent of time spent in the platform quadrant, and percent of distance travelled in the platform quadrant in the probe trial of the Morris water maze test (n = 13 per group). Data were presented as mean ± SEM. $^*P < 0.05$, $^{**}P < 0.01$ versus control mice.

3. Results

3.1. Iron exposure induced cognitive impairments

Novel object recognition task (Fig. 1A) showed that the exploration time for the novel object was shorter in iron-treated mice than in the control ones ($t = 3.922$, $P < 0.01$). The step-down passive avoidance test (Fig. 1B and C) showed that iron-treated mice reduced the latency ($t = 2.435$, $P < 0.05$) but increased the number of mistakes ($t = -2.287$, $P < 0.05$) compared to the controls. Morris water maze test showed that during the 5 consecutive days of training trials, iron-treated mice took longer escape latency than the control ones, especially on the second, fourth and fifth days of training session ($t = -2.369$, $P < 0.05$; $t = -2.295$, $P < 0.05$; $t = -2.567$, $P < 0.05$; respectively; Fig. 1D). During the probe test, iron-treated mice exhibited an increase in the probe time ($t = -4.355$, $P < 0.01$; Fig. 1F) but a decrease in the number of crossing movements ($t = 2.704$, $P < 0.05$; Fig. 1G) when comparing with the control ones. Besides, compared with the control mice, iron-treated mice showed a decrease in the percentage of time spent in target quadrant and percentage of distance travelled in target quadrant although no significant difference was found ($t = 1.495$, $P > 0.05$; $t = 1.359$, $P > 0.05$; respectively; Fig. 1H and I). The representative movement tracks of mice from different groups indicated that the iron-treated mice appeared

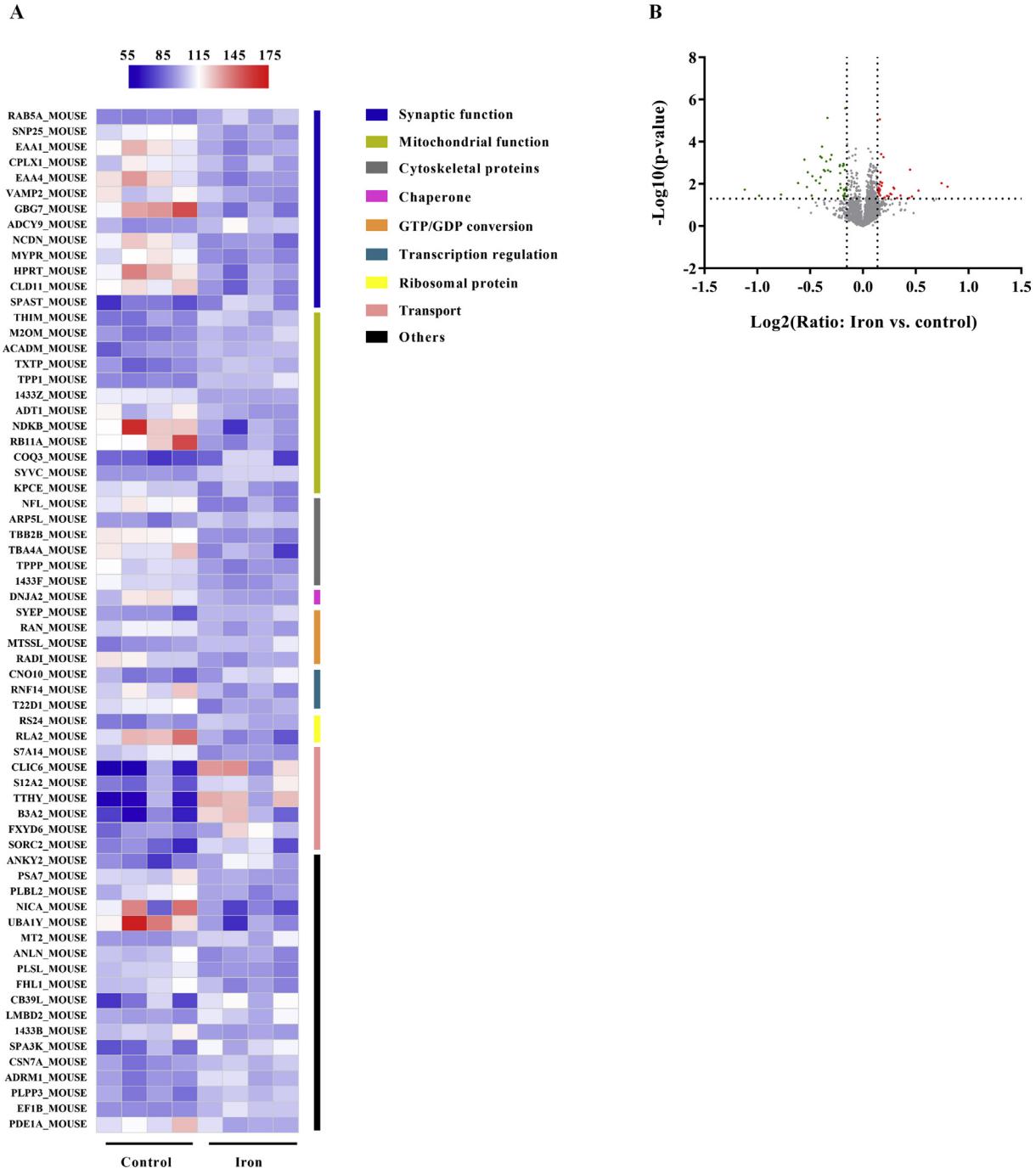

Fig. 2. Differential expression of hippocampal proteins between iron-treated and control mice. A) Heat map of altered proteins expression. B) Volcano plot for the identified proteins. Red and green dots indicate significantly up-regulated and down-regulated proteins, respectively. (For interpretation of the references to colour in this figure legend, the reader is referred to the Web version of this article.)

spatial memory impairments (Fig. 1E).

3.2. Differential expression of hippocampal proteins

In total, 4100 proteins were identified by one or more unique peptides (false discovery rate < 1%). Among the identified 4100 proteins, 66 proteins were significantly altered in the hippocampal tissues of iron-treated mice (adjusted $P < 0.05$ and ratio < 0.9 or > 1.1), which were mainly related to synaptic function, mitochondrial function, cytoskeleton, chaperone, GTP/GDP conversion, transcription regulation, ribosome, transport, and others (Fig. 2A). The names, accession numbers, fold-change levels, and P values of the differential hippocampal proteins were displayed in Supplementary Table 1.

Among 66 differential expression proteins (Fig. 2B), 36 proteins were down-regulated in iron-treated mice compared with the control ones, and 10 of them were related to synaptic function, including synaptosomal-associated protein 25 (SNAP25), complexin-1 (CPLX1), vesicle-associated membrane protein 2 (VAMP2), excitatory amino acid transporters 1 and 4 (SLC1A3 and SLC1A6), and guanine nucleotide-binding protein G(I)/G(S)/G(O) subunit gamma-7 (GNG7). Additionally, 30 proteins were up-regulated (Fig. 2B).

3.3. Enrichment analysis of differential expression proteins

To categorize the differential expression of hippocampal proteins, gene ontology analysis was performed. The 66 altered proteins were grouped based on the biological process, cellular component, and molecular function. The top 11 enriched items were displayed according to the corresponding P-values. The biological process of the identified proteins (Fig. 3A) mainly involved transport, translation, mitochondrial membrane permeability regarding apoptotic process, axonal transport of mitochondrion, axon ensheathment, neuromuscular process controlling balance, regulation of vesicle-mediated transport, axon development, cell-cell adhesion, chloride transport, and L-glutamate transport. Cellular component annotation (Fig. 3B) displayed the strong enrichments of extracellular exosome, myelin sheath, melanosome, synaptobrevin 2-SNAP-25-syntaxin-1a-complexin I complex, focal adhesion, perinuclear region of cytoplasm, ruffle, cytosol, cytoplasmic vesicle membrane, blood microparticle, and cell periphery. The results for molecular function (Fig. 3C) showed the strong enrichments of enzyme binding, protein domain specific binding, identical protein binding, structural molecule activity, syntaxin-1 binding, cadherin-mediated cell-cell adhesion, GTPase activity, actin binding, ion channel binding, protein binding, and structural constituent of ribosome.

KEGG pathway analysis (Fig. 3D) revealed that the highly enriched terms included glutamatergic synapse, synaptic vesicle cycle, purine metabolism, Fc gamma R-mediated phagocytosis, gap junction, and insulin secretion. Among proteins involved in the glutamatergic synapse pathway (Fig. S1), SLC1A3, SLC1A6, and GNG7 were down-regulated in the iron-treated mice compared with the controls, and adenylate cyclase type 9 (ADCY9) was up-regulated. However, several proteins (including SNAP25, CPLX1, and VAMP2) in the synaptic vesicle (SV) cycle pathway (Fig. S2) were down-regulated in the hippocampal proteins of iron-treated mice.

3.4. STRING analysis of protein-protein interaction networks

STRING database was used for the protein-protein interaction networks based on the differential expression proteins in relation to iron treatment (Fig. 4). Proteins regarding synaptic function and

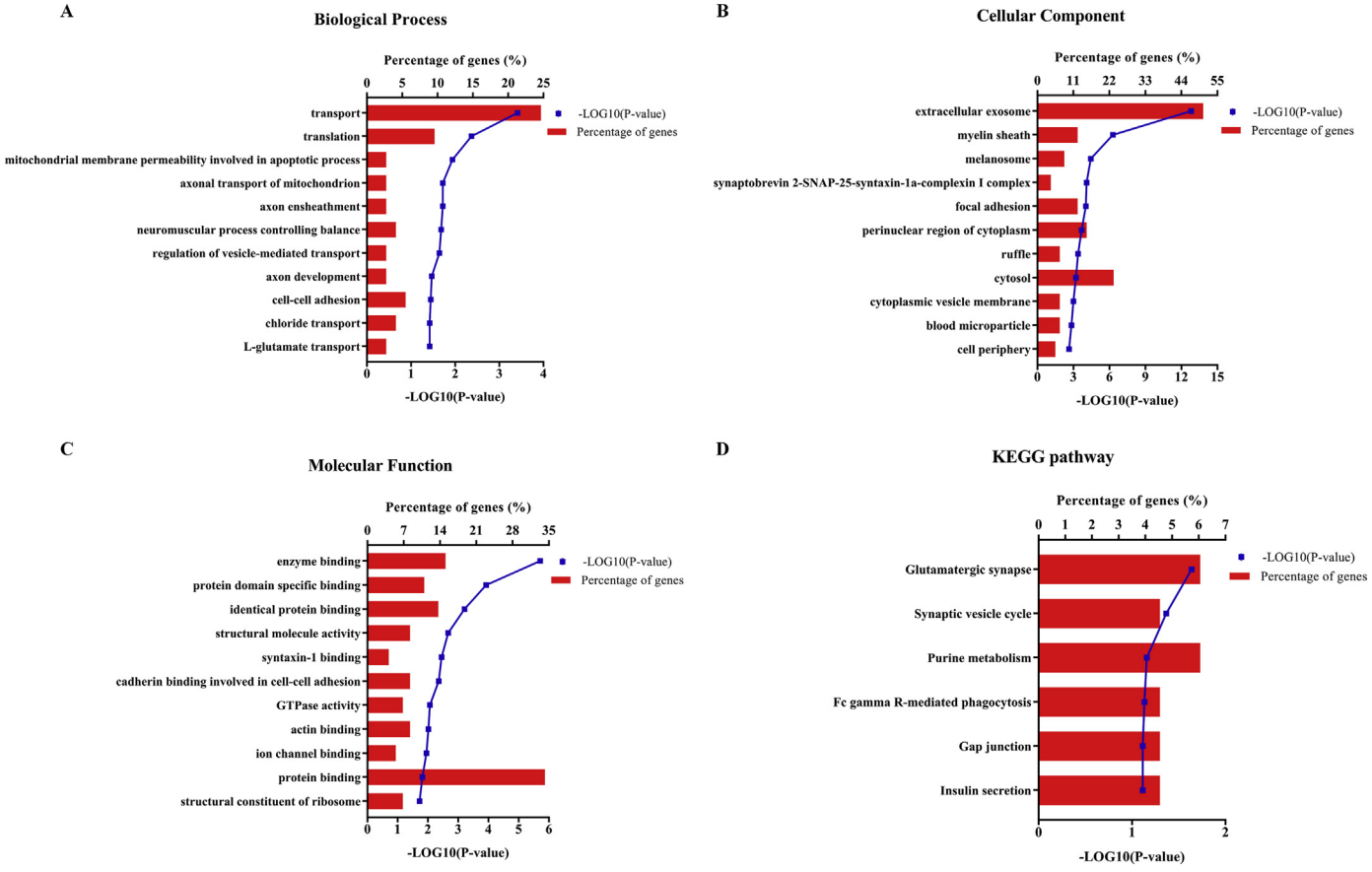

Fig. 3. Enrichment analysis of the differentially expressed hippocampal proteins in the iron-treated and untreated mice. A-C) Gene Ontology analysis of the dysregulated proteins involved in the biological process, cellular component, molecular function. D) Kyoto Encyclopedia of Genes and Genomes (KEGG) pathway analysis of the dysregulated proteins.

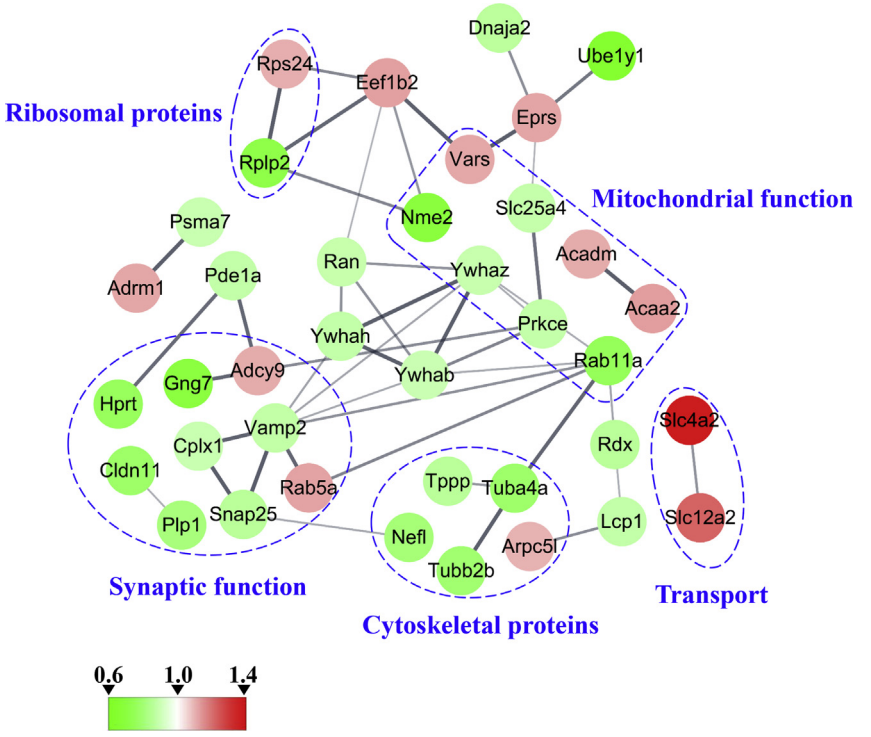

Fig. 4. Analysis of protein-protein interaction networks of the differentially expressed proteins between iron-treated and control mice. The line thickness represents the confidence scores, and thicker connection lines indicate the higher confidence of protein-protein interaction. Proteins are presented with red nodes (increased proteins) and green nodes (decreased proteins) respectively. Nodes are labeled with gene names. (For interpretation of the references to colour in this figure legend, the reader is referred to the Web version of this article.)

mitochondrial function accounted for about half of all regulated proteins. Interactions among the proteins regarding synaptic function were evident, such as proteins (SNAP25, CPLX1, and VAMP2) involved in SV cycle pathway, proteins (ADCY9 and GNG7) in the glutamatergic synapse pathway and others including hypoxanthine-guanine phosphoribosyltransferase (HPRT1), Ras-related protein Rab-5A (RAB5A), claudin-11 (CLDN11), and myelin proteolipid protein (PLP1). We found the obvious interactions of proteins involved in mitochondrial function, including 3-ketoacyl-CoA thiolase, mitochondrial (ACAA2), ADP/ATP translocase 1 (SLC25A4), medium-chain specific acyl-CoA dehydrogenase (ACADM), nucleoside diphosphate kinase B (NME2), valine-tRNA ligase (VARS), protein kinase C epsilon type (PRKCE), Ras-related protein Rab-11A (RAB11A), and 14-3-3 protein zeta/delta (YWHAZ). The other proteins were grouped into cytoskeletal proteins (15.8%), ribosomal proteins (5.3%), transport protein (5.3%) and so on.

3.5. Differential expression of representative proteins

Based on the functional analysis, the scaled abundances of nine representative proteins were further analyzed, including synapse-related proteins SNAP25, CPLX1, VAMP2, and neurochondrin (NCDN); mitochondria-associated proteins SLC25A4 and YWHAZ; cytoskeleton proteins neurofilament light polypeptide (NEFL), tubulin beta-2B chain (TUBB2B) as well as tubulin alpha-4A chain (TUBA4A) (Fig. 5A–C).

3.6. Validation of differential expression protein

To confirm proteomic data, the further verification of differential expression of synaptic protein SNAP25 was performed using Western blot. SNAP25 protein was selected to be further analyzed based on bioinformatics analysis including KEGG pathway analysis, protein-protein interaction networks as well as fold-change levels of the differential hippocampal proteins. The results of Western blot was in accordance with those of proteomic analysis, showing that expression of SNAP25 protein was down-regulated in the iron-treated mice compared to the control ones ($t = 2.470$, $P < 0.05$; Fig. 6A–C).

4. Discussion

The current study found that after long-term iron exposure, mice exhibited cognitive impairments accompanying the alterations of hippocampal proteins. The differentially expressed proteins were largely relevant to synaptic function, mitochondrial function, cytoskeleton, etc. The downregulation of SNAP25, a significant synaptic protein located in the SV cycle, was further verified by Western blot in the iron-treated mice.

The analysis of data obtained from the behavioral tests consistently demonstrated that iron administration could induce cognitive impairments of the mice. The results were in line with previous studies, which suggested that iron supplementation via drinking water (10 mg/mL for 3 months, or 10 mg/L for 11 months) could exacerbate defects in spatial learning and memory in different mouse models of AD (amyloid precursor protein (APP)/presenilin 1 (PS1) transgenic mice or Tg2576 mice) (Guo et al., 2013; Railey et al., 2011). Another study also reported that intraperitoneal injection of Fe^{2+} (10 mg/kg, twice a week, for 4 weeks) could hasten cognitive decline in APP/PS1 mice by a novel object recognition test (Becerril-Ortega et al., 2014).

Proteomics has been recently applied to explore the toxic effects of various chemicals (Revel et al., 2017; Wei et al., 2018; Yan et al., 2018), because proteomic methods can provide information about the overall response of the model systems to toxins, and help to comprehensively understand mechanisms of toxic substances based on the detailed bioinformatics analysis. Whereas, little *in vivo* studies regarding iron neurotoxicity with proteomics approaches have been reported. The results indicated that iron induced the alterations of hippocampal proteins from the mice, showing the dysregulation of proteins involved in the synaptic function, mitochondrial function, and cytoskeleton.

We found that iron treatment induced the decreased synaptic proteins in the hippocampal neurons, such as SNAP25, CPLX1, VAMP2, and NCDN. SNAP25, CPLX1, and VAMP2 proteins in the SV cycle pathway are essential to neuronal communications, because the exocytosis of SVs mediated the neurotransmitter release from presynaptic nerve terminal (Wang et al., 2017a). While SNAP25 can provide the driving force for vesicle docking and fusion, abnormalities in its expression and structure can induce multiple neurological disorders

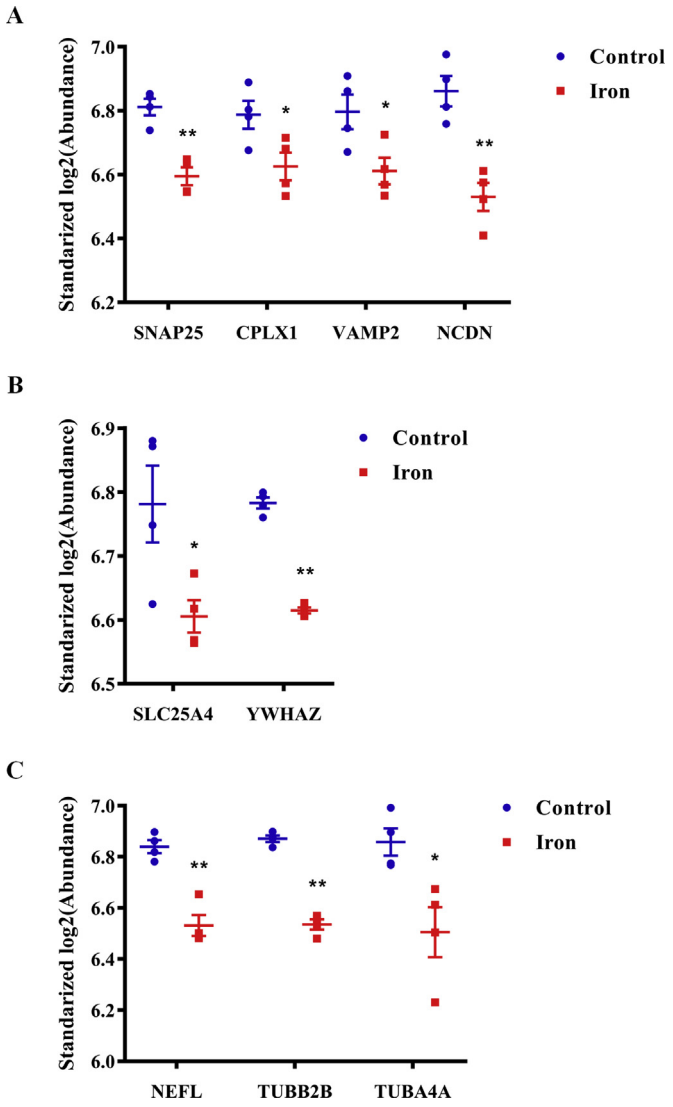

Fig. 5. Differential expression of representative proteins in iron-treated mice. A) Abnormal expression of proteins relevant to synaptic function. B) Abnormal expression of proteins relevant to mitochondrial function. C) Abnormal expression of proteins relevant to cytoskeleton. Data were presented as mean ± SEM. $^{*}P < 0.05$, $^{**}P < 0.01$ versus the control mice. n = 4 in each group. **Abbreviations**: SNAP25, synaptosomal-associated protein 25; CPLX1, complexin-1; VAMP2, vesicle-associated membrane protein 2; NCDN, neurochondrin; SLC25A4, ADP/ATP translocase 1; YWHAZ, 14-3-3 protein zeta/delta; NEFL, neurofilament light polypeptide; TUBB2B, tubulin beta-2B chain; TUBA4A, tubulin alpha-4A chain.

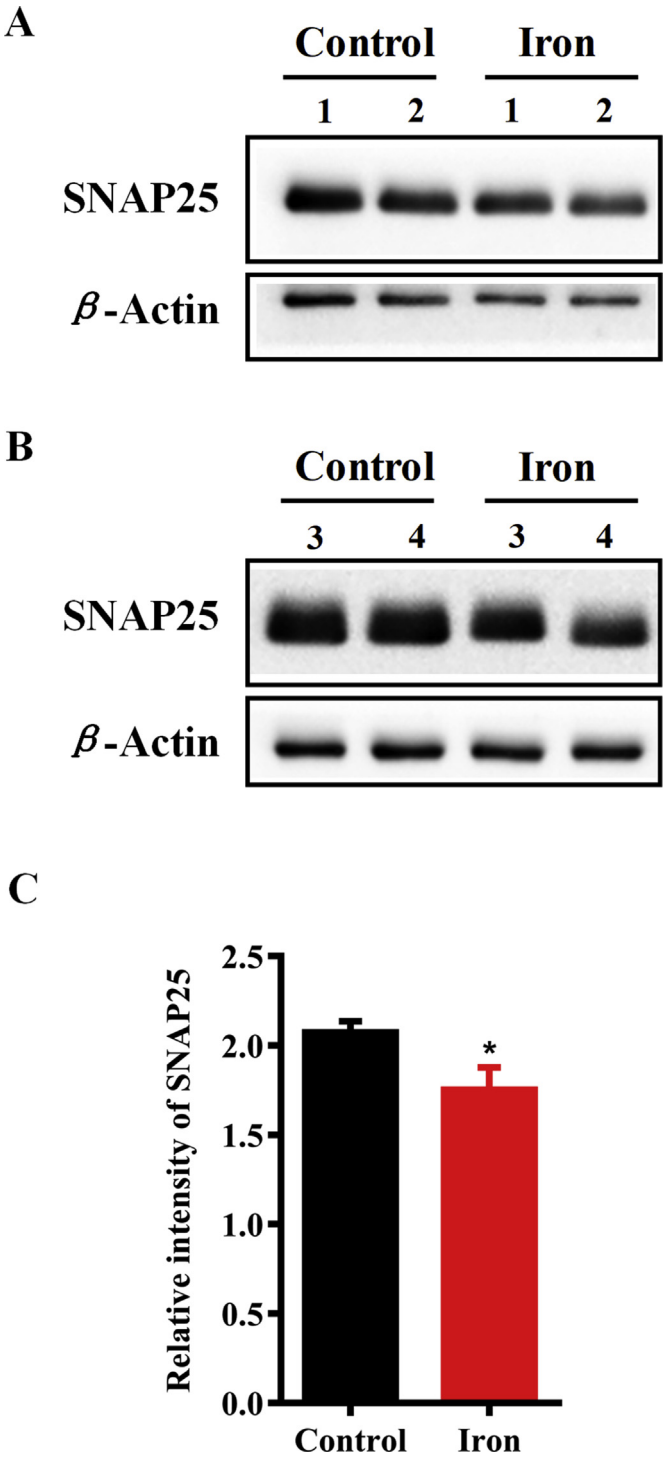

Fig. 6. Validation of differentially expressed protein SNAP25 was further performed using Western blot analysis. Data were presented as mean ± SEM. $^{*}P < 0.05$ versus the control mice. n = 4 for each group. **Abbreviations**: SNAP25, synaptosomal-associated protein 25.

including AD, attention deficient hyperactivity disorder, schizophrenia (Noor and Zahid, 2017). On the one hand, SNAP25 may play significant roles in presynaptic events, including the interaction with various synaptic proteins, formations of several complexes and alterations of presynaptic plasma membrane dynamics. On the other hand, SNAP25 was found to participate in the regulation of spine morphogenesis, indicating that SNAP25 may be an important role-player in postsynaptic events as well (Karmakar et al., 2019). Complexins (Cplxs) which cooperate with soluble *N*-ethylmaleimide-sensitive factor attachment protein receptors (SNARE) complexes, play an important role in the regulation of SV fusion. A study in *Cplx1* knock-out mice showed that CPLX1 could enhance both spontaneous and evoked transmitter releases, stabilize newly primed synaptic vesicles and prevent premature release of them (Chang et al., 2015). Our previous study showed that the downregulation of CPLX1 in hippocampus contributed to spatial memory impairment in triple transgenic mouse model of AD (Ying et al., 2017). Additionally, expression level of VAMP2 can affect synaptic transmission, vesicle fusion, endocytosis, and neurotransmitter release. The downregulation of VAMP2 was found in the brains of AD patients (Pham et al., 2010). A recent study reported that mutations of *VAMP2* could affect synaptic membrane fusion and impair the development and functions of human brain (Salpietro et al., 2019). In knockout mice lacking VAMP2, spontaneous synaptic vesicle fusion and

fast Ca^{2+}-triggered fusion were markedly decreased (Schoch et al., 2001). Besides, the shape and size of the vesicles in synapses altered in the *Vamp2*-deficient mice, showing a defect in the endocytosis (Deak et al., 2004). NCDN plays an essential role in synaptic plasticity, neurite outgrowth, and regulation of signal transduction. Additionally, it may have the potential as a therapeutic target for the neurodegenerative disease spinal muscular atrophy (Thompson et al., 2018). Taken together, our findings revealed the correlations between iron-induced memory impairment and the downregulations of SV cycle-related proteins including SNAP25, CPLX1, VAMP2, and other synapse-associated proteins.

Dysfunction of iron homeostasis may induce energy supply deficiency and mitochondrial fragmentation, thus affect mitochondrial function (Huang et al., 2018). The proteomic data showed that oral iron treatment could downregulate mitochondria-associated proteins in the mice, including SLC25A4 and 14-3-3 protein zeta/delta (YWHAZ). SLC25A4 located in the inner membrane of mitochondria is one of the significant enzymes in ATP/ADP exchange, and abnormal SLC25A4 activity can lead to cellular dysfunction and even cell death (Sari et al., 2010). The *Slc25a4*-deficient mice had impaired mitochondrial exchange of ATP/ADP, increased production of mitochondrial reactive oxygen species and decreased tissue respiration stimulated by ADP (Esposito et al., 1999). The studies found that SLC25A4 may be a regulatory element of the mitochondrial permeability transition pore involved in the regulated cell death (Clemencon et al., 2013; Kato et al., 2018). Abundant 14-3-3 proteins in the brain play key roles in lots of cellular processes, such as protein synthesis and trafficking, signal transduction, cell cycle as well as the regulation of metabolism. They have been connected with a number of neurological diseases involving AD, amyotrophic lateral sclerosis, Parkinson's disease (Iwamoto et al., 2014; Smani et al., 2018). The 14-3-3 proteins can bind to apoptotic signal transducing proteins and mitochondrial apoptotic proteins, and then directly inhibit apoptosis (Jeon et al., 2016). A study found that the depletion of 14-3-3 zeta could lead to endoplasmic reticulum stress and cell death in mouse hippocampal cultures (Murphy et al., 2008), while another one reported that overexpression of 14-3-3 zeta may protect the mouse hippocampus against neuronal death induced by endoplasmic reticulum stress and seizure (Brennan et al., 2013). The present study clearly showed the reduced expression of SLC25A4 and YWHAZ in the iron-treated mice as compared with the control ones, indicating that abnormal expression of mitochondria-related proteins could be involved in the cognitive dysfunction induced by iron administration.

We found that iron treatment could downregulate expression of major cytoskeletal proteins in the hippocampus of mice, including NEFL, tubulin beta-2B chain (TUBB2B), tubulin alpha-4A chain (TUBA4A). NEFL as a component of the neuronal cytoskeleton is predominantly expressed in large-caliber myelinated axons, and changes of NEFL expression are associated with brain atrophy and brain damage in various neurodegenerative disorders (Byrne et al., 2018; Preische et al., 2019; Schreiber et al., 2018). An earlier study found that knocking out the *Nefl* gene in the mice could eliminate neurofilaments in myelinated peripheral nervous system axons, which may affect their normal enlargements during the development (Zhu et al., 1997). A study in the APP/PS1 *Nefl*$^{-/-}$ mice showed that the deletion of *Nefl* gene could increase the accumulation of neocortical amyloid-beta, synapse vulnerability close to plaques and microgliosis, indicating the protective role of NEFL in AD (Fernandez-Martos et al., 2015). Microtubule is composed of tubulin (α and β) subunits. It is the second major component of the axonal cytoskeleton and plays significant roles in cellular structure (Teunissen et al., 2005). Recent studies have revealed the connection between neuronal cytoskeletal damage and neurodegeneration, and cytoskeleton is considered as a new therapeutic target for neurodegenerative diseases (Eira et al., 2016). Collectively, our results indicate that decreased levels of NEFL and tubulin may contribute to iron neurotoxicity regarding disrupting axonal integrity.

In addition, iron treatment altered the levels of proteins related to iron metabolism and oxidative stress in the mice. For instance, metallothionein-2 (MT2) was upregulated in the iron-treated mice. Metallothioneins (MTs) as a superfamily of low-molecular weight proteins could participate in various physical processes, including metabolisms (transport and storage) of iron, copper and zinc, detoxification of cadmium and mercury, and protection against oxidative damage to dopaminergic neurons (Comes et al., 2019; Park and Yu, 2013; Schuermann et al., 2015). MTs as thiol rich metal binding proteins are able to regulate the distributions of metals in body and donate required metals to enzymes or transcription factors (Joneidi et al., 2019). The reasons for the potential antioxidant activity of MTs may be the direct scavenging of destructive free radicals, complex reactions involving redox active transition metals and the alteration of zinc homeostasis (Formigari et al., 2007; Wang et al., 2017b). Owing to the fact that metals and oxidative stress affect the expression of MTs, the increased

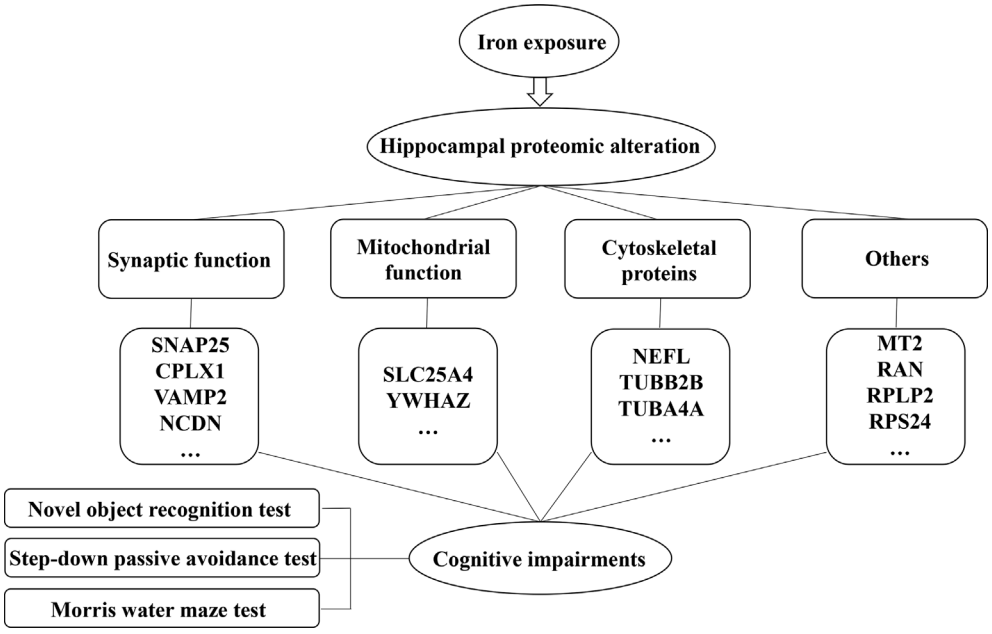

Fig. 7. Schematic diagram demonstrating the effects of iron treatment on cognitive function and hippocampal proteome in mice. Iron treatment induced alterations in hippocampal proteome, including proteins related to synaptic function, mitochondrial function, cytoskeleton, etc. The changes of expression levels of these key proteins may contribute to iron-induced memory impairments as observed. **Abbreviations**: SNAP25, synaptosomal-associated protein 25; CPLX1, complexin-1; VAMP2, vesicle-associated membrane protein 2; NCDN, neurochondrin; SLC25A4, ADP/ATP translocase 1; YWHAZ, 14-3-3 protein zeta/delta; NEFL, neurofilament light polypeptide; TUBB2B, tubulin beta-2B chain; TUBA4A, tubulin alpha-4A chain; MT2, metallothionein-2; RAN, GTP-binding nuclear protein Ran; RPLP2, 60S acidic ribosomal protein P2; RPS24, 40S ribosomal protein S24.

MT2 levels in the iron-treated mice may be a compensation response of the accumulation of free radicals.

5. Conclusions

Long-term iron exposure induced the cognitive defects accompanying the alterations of certain hippocampal proteins in the mice, particularly involving synapse-associated proteins (SNAP25, CPLX1, VAMP2, NCDN), mitochondria-related proteins (SLC25A4, YWHAZ), and cytoskeleton proteins (NEFL, TUBB2B, TUBA4A) (summarized in Fig. 7). The alterations of hippocampal synaptic, mitochondrial, and cytoskeletal proteins may be involved in the iron-induced memory impairment. Our results may provide new insights into the molecular mechanisms of iron neurotoxicity. Further studies are needed to elucidate the roles and relevant molecular mechanisms of the identified key proteins in iron-mediated cognitive impairments.

Conflicts of interest

All authors declare they have no conflict of interest.

Acknowledgements

This work was supported by National Natural Science Foundation of China (81673134, 81401570) and Sanming Project of Medicine in Shenzhen (SZSM201611090).

Appendix A. Supplementary data

Supplementary data to this article can be found online at https://doi.org/10.1016/j.fct.2019.05.038.

Transparency document

Transparency document related to this article can be found online at https://doi.org/10.1016/j.fct.2019.05.038

References

Acosta-Cabronero, J., Cardenas-Blanco, A., Betts, M.J., Butryn, M., Valdes-Herrera, J.P., Galazky, I., Nestor, P.J., 2017. The whole-brain pattern of magnetic susceptibility perturbations in Parkinson's disease. Brain 140, 118–131.

Agrawal, S., Berggren, K.L., Marks, E., Fox, J.H., 2017. Impact of high iron intake on cognition and neurodegeneration in humans and in animal models: a systematic review. Nutr. Rev. 75, 456–470.

Andrade, V.M., Aschner, M., Marreilha Dos Santos, A.P., 2017. Neurotoxicity of metal mixtures. Adv. Neurobiol. 18, 227–265.

Ayton, S., Fazlollahi, A., Bourgeat, P., Raniga, P., Ng, A., Lim, Y.Y., Diouf, I., Farquharson, S., Fripp, J., Ames, D., Doecke, J., Desmond, P., Ordidge, R., Masters, C.L., Rowe, C.C., Maruff, P., Villemagne, V.L., Australian Imaging B, Lifestyle Research G, Salvado, O., Bush, A.I., 2017. Cerebral quantitative susceptibility mapping predicts amyloid-beta-related cognitive decline. Brain 140, 2112–2119.

Becerril-Ortega, J., Bordji, K., Freret, T., Rush, T., Buisson, A., 2014. Iron overload accelerates neuronal amyloid-beta production and cognitive impairment in transgenic mice model of Alzheimer's disease. Neurobiol. Aging 35, 2288–2301.

Bereczki, E., Branca, R.M., Francis, P.T., Pereira, J.B., Baek, J.H., Hortobagyi, T., Winblad, B., Ballard, C., Lehtio, J., Aarsland, D., 2018. Synaptic markers of cognitive decline in neurodegenerative diseases: a proteomic approach. Brain 141, 582–595.

Brennan, G.P., Jimenez-Mateos, E.M., McKiernan, R.C., Engel, T., Tzivion, G., Henshall, D.C., 2013. Transgenic overexpression of 14-3-3 zeta protects hippocampus against endoplasmic reticulum stress and status epilepticus in vivo. PLoS One 8, e54491.

Byrne, L.M., Rodrigues, F.B., Johnson, E.B., Wijeratne, P.A., De Vita, E., Alexander, D.C., Palermo, G., Czech, C., Schobel, S., Scahill, R.I., Heslegrave, A., Zetterberg, H., Wild, E.J., 2018. Evaluation of mutant huntingtin and neurofilament proteins as potential markers in Huntington's disease. Sci. Transl. Med. 10.

Chang, S., Reim, K., Pedersen, M., Neher, E., Brose, N., Taschenberger, H., 2015. Complexin stabilizes newly primed synaptic vesicles and prevents their premature fusion at the mouse calyx of held synapse. J. Neurosci. 35, 8272–8290.

Chen, L.L., Huang, Y.J., Cui, J.T., Song, N., Xie, J., 2019. Iron dysregulation in Parkinson's disease: focused on the autophagy-lysosome pathway. ACS Chem. Neurosci. 10, 863–871.

Clemencon, B., Babot, M., Trezeguet, V., 2013. The mitochondrial ADP/ATP carrier (SLC25 family): pathological implications of its dysfunction. Mol. Asp. Med. 34, 485–493.

Comes, G., Fernandez-Gayol, O., Molinero, A., Giralt, M., Capdevila, M., Atrian, S., Hidalgo, J., 2019. Mouse metallothionein-1 and metallothionein-2 are not biologically interchangeable in an animal model of multiple sclerosis. EAE. Metallomics 11, 327–337.

Conde, J.R., Streit, W.J., 2006. Microglia in the aging brain. J. Neuropathol. Exp. Neurol. 65, 199–203.

Deak, F., Schoch, S., Liu, X., Sudhof, T.C., Kavalali, E.T., 2004. Synaptobrevin is essential for fast synaptic-vesicle endocytosis. Nat. Cell Biol. 6, 1102–1108.

Eira, J., Silva, C.S., Sousa, M.M., Liz, M.A., 2016. The cytoskeleton as a novel therapeutic target for old neurodegenerative disorders. Prog. Neurobiol. 141, 61–82.

Esposito, L.A., Melov, S., Panov, A., Cottrell, B.A., Wallace, D.C., 1999. Mitochondrial disease in mouse results in increased oxidative stress. Proc. Natl. Acad. Sci. U. S. A. 96, 4820–4825.

Faraco, G., Brea, D., Garcia-Bonilla, L., Wang, G., Racchumi, G., Chang, H., Buendia, I., Santisteban, M.M., Segarra, S.G., Koizumi, K., Sugiyama, Y., Murphy, M., Voss, H., Anrather, J., Iadecola, C., 2018. Dietary salt promotes neurovascular and cognitive dysfunction through a gut-initiated TH17 response. Nat. Neurosci. 21, 240–249.

Farrall, A.J., Wardlaw, J.M., 2009. Blood-brain barrier: ageing and microvascular disease–systematic review and meta-analysis. Neurobiol. Aging 30, 337–352.

Fernandez-Martos, C.M., King, A.E., Atkinson, R.A., Woodhouse, A., Vickers, J.C., 2015. Neurofilament light gene deletion exacerbates amyloid, dystrophic neurite, and synaptic pathology in the APP/PS1 transgenic model of Alzheimer's disease. Neurobiol. Aging 36, 2757–2767.

Formigari, A., Santon, A., Irato, P., 2007. Efficacy of zinc treatment against iron-induced toxicity in rat hepatoma cell line H4-II-E-C3. Liver Int. 27, 120–127.

Fredriksson, A., Schroder, N., Eriksson, P., Izquierdo, I., Archer, T., 1999. Neonatal iron exposure induces neurobehavioural dysfunctions in adult mice. Toxicol. Appl. Pharmacol. 159, 25–30.

Gao, G., Chang, Y.Z., 2014. Mitochondrial ferritin in the regulation of brain iron homeostasis and neurodegenerative diseases. Front. Pharmacol. 5, 19.

Gokce, E., Andrews, G.L., Dean, R.A., Muddiman, D.C., 2011. Increasing proteome coverage with offline RP HPLC coupled to online RP nanoLC-MS. J. Chromatogr. B. Analyt. Technol. Biomed. Life Sci. 879, 610–614.

Guo, C., Wang, T., Zheng, W., Shan, Z.Y., Teng, W.P., Wang, Z.Y., 2013. Intranasal deferoxamine reverses iron-induced memory deficits and inhibits amyloidogenic APP processing in a transgenic mouse model of Alzheimer's disease. Neurobiol. Aging 34, 562–575.

Huang, X.T., Liu, X., Ye, C.Y., Tao, L.X., Zhou, H., Zhang, H.Y., 2018. Iron-induced energy supply deficiency and mitochondrial fragmentation in neurons. J. Neurochem. 147, 816–830.

Iwamoto, M., Miura, Y., Tsumoto, H., Tanaka, Y., Morisawa, H., Endo, T., Toda, T., 2014. Antioxidant effects of carnitine supplementation on 14-3-3 protein isoforms in the aged rat hippocampus detected using fully automated two-dimensional chip gel electrophoresis. Free Radic. Res. 48, 1409–1416.

Jeon, S.J., Sung, J.H., Koh, P.O., 2016. Hyperglycemia decreases expression of 14-3-3 proteins in an animal model of stroke. Neurosci. Lett. 626, 13–18.

Jiang, H., Wang, J., Rogers, J., Xie, J., 2017. Brain iron metabolism dysfunction in Parkinson's disease. Mol. Neurobiol. 54, 3078–3101.

Joneidi, Z., Mortazavi, Y., Memari, F., Roointan, A., Chahardouli, B., Rostami, S., 2019. The impact of genetic variation on metabolism of heavy metals: genetic predisposition? Biomed. Pharmacother. 113, 108642.

Karmakar, S., Sharma, L.G., Roy, A., Patel, A., Pandey, L.M., 2019. Neuronal SNARE complex: a protein folding system with intricate protein-protein interactions, and its common neuropathological hallmark. SNAP25. Neurochem. Int. 122, 196–207.

Kato, T.M., Kubota-Sakashita, M., Fujimori-Tonou, N., Saitow, F., Fuke, S., Masuda, A., Itohara, S., Suzuki, H., Kato, T., 2018. Ant1 mutant mice bridge the mitochondrial and serotonergic dysfunctions in bipolar disorder. Mol. Psychiatry 23, 2039–2049.

Lee, D.G., Park, J., Lee, H.S., Lee, S.R., Lee, D.S., 2016. Iron overload-induced calcium signals modulate mitochondrial fragmentation in HT-22 hippocampal neuron cells. Toxicology 365, 17–24.

Maaroufi, K., Ammari, M., Jeljeli, M., Roy, V., Sakly, M., Abdelmelek, H., 2009. Impairment of emotional behavior and spatial learning in adult Wistar rats by ferrous sulfate. Physiol. Behav. 96, 343–349.

Murphy, N., Bonner, H.P., Ward, M.W., Murphy, B.M., Prehn, J.H., Henshall, D.C., 2008. Depletion of 14-3-3 zeta elicits endoplasmic reticulum stress and cell death, and increases vulnerability to kainate-induced injury in mouse hippocampal cultures. J. Neurochem. 106, 978–988.

Noor, A., Zahid, S., 2017. A review of the role of synaptosomal-associated protein 25 (SNAP-25) in neurological disorders. Int. J. Neurosci. 127, 805–811.

Park, J., Lee, D.G., Kim, B., Park, S.J., Kim, J.H., Lee, S.R., Chang, K.T., Lee, H.S., Lee, D.S., 2015. Iron overload triggers mitochondrial fragmentation via calcineurin-sensitive signals in HT-22 hippocampal neuron cells. Toxicology 337, 39–46.

Park, Y., Yu, E., 2013. Expression of metallothionein-1 and metallothionein-2 as a prognostic marker in hepatocellular carcinoma. J. Gastroenterol. Hepatol. 28, 1565–1572.

Peto, M.V., 2010. Aluminium and iron in humans: bioaccumulation, pathology, and removal. Rejuvenation Res. 13, 589–598.

Pham, E., Crews, L., Ubhi, K., Hansen, L., Adame, A., Cartier, A., Salmon, D., Galasko, D., Michael, S., Savas, J.N., Yates, J.R., Glabe, C., Masliah, E., 2010. Progressive accumulation of amyloid-beta oligomers in Alzheimer's disease and in amyloid precursor protein transgenic mice is accompanied by selective alterations in synaptic scaffold proteins. FEBS J. 277, 3051–3067.

Pike, N., 2011. Using false discovery rates for multiple comparisons in ecology and evolution. Methods Ecol. Evol. 2, 278–282.

Preische, O., Schultz, S.A., Apel, A., Kuhle, J., Kaeser, S.A., Barro, C., Graber, S., Kuder-Buletta, E., LaFougere, C., Laske, C., Voglein, J., Levin, J., Masters, C.L., Martins, R.,

Schofield, P.R., Rossor, M.N., Graff-Radford, N.R., Salloway, S., Ghetti, B., Ringman, J.M., Noble, J.M., Chhatwal, J., Goate, A.M., Benzinger, T.L.S., Morris, J.C., Bateman, R.J., Wang, G., Fagan, A.M., McDade, E.M., Gordon, B.A., Jucker, M., Dominantly Inherited Alzheimer, N., 2019. Serum neurofilament dynamics predicts neurodegeneration and clinical progression in presymptomatic Alzheimer's disease. Nat. Med. 25, 277–283.

Pretorius, L., Kell, D.B., Pretorius, E., 2018. Iron dysregulation and dormant microbes as causative agents for impaired blood rheology and pathological clotting in Alzheimer's type dementia. Front. Neurosci. 12, 851.

Railey, A.M., Groeber, C.M., Flinn, J.M., 2011. The effect of metals on spatial memory in a transgenic mouse model of Alzheimer's disease. J. Alzheimer's Dis. 24, 375–381.

Revel, M., Chatel, A., Mouneyrac, C., 2017. Omics tools: new challenges in aquatic nanotoxicology? Aquat. Toxicol. 193, 72–85.

Salpietro, V., Malintan, N.T., Llano-Rivas, I., Spaeth, C.G., Efthymiou, S., Striano, P., Vandrovcova, J., Cutrupi, M.C., Chimenz, R., David, E., Di Rosa, G., Marce-Grau, A., Raspall-Chaure, M., Martin-Hernandez, E., Zara, F., Minetti, C., Deciphering Developmental Disorders S, Group S.S., Bello, O.D., De Zorzi, R., Fortuna, S., Dauber, A., Alkhawaja, M., Sultan, T., Mankad, K., Vitobello, A., Thomas, Q., Mau-Them, F.T., Faivre, L., Martinez-Azorin, F., Prada, C.E., Macaya, A., Kullmann, D.M., Rothman, J.E., Krishnakumar, S.S., Houlden, H., 2019. Mutations in the neuronal vesicular SNARE VAMP2 affect synaptic membrane fusion and impair human neurodevelopment. Am. J. Hum. Genet. 104, 721–730.

Sari, Y., Zhang, M., Mechref, Y., 2010. Differential expression of proteins in fetal brains of alcohol-treated prenatally C57BL/6 mice: a proteomic investigation. Electrophoresis 31, 483–496.

Schoch, S., Deak, F., Konigstorfer, A., Mozhayeva, M., Sara, Y., Sudhof, T.C., Kavalali, E.T., 2001. SNARE function analyzed in synaptobrevin/VAMP knockout mice. Science 294, 1117–1122.

Schreiber, S., Spotorno, N., Schreiber, F., Acosta-Cabronero, J., Kaufmann, J., Machts, J., Debska-Vielhaber, G., Garz, C., Bittner, D., Hensiek, N., Dengler, R., Petri, S., Nestor, P.J., Vielhaber, S., 2018. Significance of CSF NfL and tau in ALS. J. Neurol. 265, 2633–2645.

Schroder, N., Figueiredo, L.S., de Lima, M.N., 2013. Role of brain iron accumulation in cognitive dysfunction: evidence from animal models and human studies. J. Alzheimer's Dis. 34, 797–812.

Schuermann, A., Helker, C.S., Herzog, W., 2015. Metallothionein 2 regulates endothelial cell migration through transcriptional regulation of vegfc expression. Angiogenesis 18, 463–475.

Smani, D., Sarkar, S., Raymick, J., Kanungo, J., Paule, M.G., Gu, Q., 2018. Downregulation of 14-3-3 proteins in a kainic acid-induced neurotoxicity model. Mol. Neurobiol. 55, 122–129.

Teunissen, C.E., Dijkstra, C., Polman, C., 2005. Biological markers in CSF and blood for axonal degeneration in multiple sclerosis. Lancet Neurol. 4, 32–41.

Thompson, L.W., Morrison, K.D., Shirran, S.L., Groen, E.J.N., Gillingwater, T.H., Botting, C.H., Sleeman, J.E., 2018. Neurochondrin interacts with the SMN protein suggesting a novel mechanism for spinal muscular atrophy pathology. J. Cell Sci. 131.

Tyanova, S., Temu, T., Sinitcyn, P., Carlson, A., Hein, M.Y., Geiger, T., Mann, M., Cox, J., 2016. The Perseus computational platform for comprehensive analysis of (prote) omics data. Nat. Methods 13, 731–740.

Vorhees, C.V., Williams, M.T., 2006. Morris water maze: procedures for assessing spatial and related forms of learning and memory. Nat. Protoc. 1, 848–858.

Wang, C., Zhao, D., Shah, S.Z.A., Yang, W., Li, C., Yang, L., 2017a. Proteome analysis of potential synaptic vesicle cycle Biomarkers in the cerebrospinal fluid of patients with sporadic creutzfeldt-jakob disease. Mol. Neurobiol. 54, 5177–5191.

Wang, X., Wu, X., Liu, Q., Kong, G., Zhou, J., Jiang, J., Wu, X., Huang, Z., Su, W., Zhu, Q., 2017b. Ketogenic metabolism inhibits histone deacetylase (HDAC) and reduces oxidative stress after spinal cord injury in rats. Neuroscience 366, 36–43.

Ward, R.J., Zucca, F.A., Duyn, J.H., Crichton, R.R., Zecca, L., 2014. The role of iron in brain ageing and neurodegenerative disorders. Lancet Neurol. 13, 1045–1060.

Wei, Y., Zeng, B., Zhang, H., Chen, C., Wu, Y., Wang, N., Wu, Y., Zhao, D., Zhao, Y., Iqbal, J., Shen, L., 2018. Comparative proteomic analysis of fluoride treated rat bone provides new insights into the molecular mechanisms of fluoride toxicity. Toxicol. Lett. 291, 39–50.

Weinreb, O., Mandel, S., Youdim, M.B.H., Amit, T., 2013. Targeting dysregulation of brain iron homeostasis in Parkinson's disease by iron chelators. Free Radic. Biol. Med. 62, 52–64.

Xu, B., Zhang, Y., Zhan, S., Wang, X., Zhang, H., Meng, X., Ge, W., 2018. Proteomic profiling of brain and testis reveals the diverse changes in ribosomal proteins in fmr1 knockout mice. Neuroscience 371, 469–483.

Yan, X., He, B., Hu, L., Gao, J., Chen, S., Jiang, G., 2018. Insight into the endocrine disrupting effect and cell response to butyltin compounds in H295R cell: evaluated with proteomics and bioinformatics analysis. Sci. Total Environ. 628–629, 1489–1496.

Ying, M., Sui, X., Zhang, Y., Sun, Q., Qu, Z., Luo, X., Chang, R.C., Ni, J., Liu, J., Yang, X., 2017. Identification of novel key molecules involved in spatial memory impairment in triple transgenic mice of Alzheimer's disease. Mol. Neurobiol. 54, 3843–3858.

Zhou, X., Xiao, W., Su, Z., Cheng, J., Zheng, C., Zhang, Z., Wang, Y., Wang, L., Xu, B., Li, S., Yang, X., Pui Man Hoi, M., 2019. Hippocampal proteomic alteration in triple transgenic mouse model of Alzheimer's disease and implication of PINK 1 regulation in donepezil treatment. J. Proteome Res. 18, 1542–1552.

Zhu, Q., Couillard-Despres, S., Julien, J.P., 1997. Delayed maturation of regenerating myelinated axons in mice lacking neurofilaments. Exp. Neurol. 148, 299–316.

Zivadinov, R., Tavazzi, E., Bergsland, N., Hagemeier, J., Lin, F., Dwyer, M.G., Carl, E., Kolb, C., Hojnacki, D., Ramasamy, D., Durfee, J., Weinstock-Guttman, B., Schweser, F., 2018. Brain iron at quantitative MRI is associated with disability in multiple sclerosis. Radiology 289, 487–496.